DOI: 10.1002/ejic.200900173

Water-Soluble *Ultra Small* Paramagnetic or Superparamagnetic Metal Oxide Nanoparticles for Molecular MR Imaging

Ja Young Park,[a] Eun Sook Choi,[a] Myung Ju Baek,[b] Gang Ho Lee,*[a,b] Seungtae Woo,[c] and Yongmin Chang*[c]

Keywords: Colloids / Imaging agents / Nanostructures / Nanotechnology

A simple and general one-pot synthesis for water-soluble ligand-coated *ultra small* paramagnetic or superparamagnetic metal oxide nanoparticles with average particle diameters ($d_{av.}$) that range from 1–3 nm has been developed and used in molecular magnetic resonance (MR) imaging. The iron oxide, manganese oxide, and gadolinium oxide nanoparticles are coated with various hydrophilic and biocompatible ligands. We found that the ligand-coated *ultra small* gadolinium oxide nanoparticles are the superior candidates for use as T_1 MRI contrast agents.

Introduction

One of the final goals in clinical molecular magnetic resonance (MR) imaging is to achieve both highly sensitive and target-specific detection of diseases by help of magnetic resonance imaging (MRI) contrast agents. To accomplish this, the MRI contrast agent should possess as high as possible relaxivity and as small as possible size. Nanotechnology-based MRI contrast agents can possess high relaxivities, and thus paramagnetic or superparamagnetic nanoparticles have been intensively investigated so far.[1–14] However, large nanoparticles have a very poor target-specific capability because they are mostly accumulated in the liver as demonstrated with the iron oxide nanoparticles.[3] Therefore, the development of *ultra small* nanoparticles with high relaxivities is necessary. In this work, we present a simple and general one-pot (or one-step) synthesis for hydrophilic and biocompatible ligand-coated *ultra small* paramagnetic or superparamagnetic metal oxide nanoparticles with average particle diameters ($d_{av.}$) that range from 1–3 nm. To the best of our knowledge, these ligand-coated *ultra small* metal oxide nanoparticles are the smallest synthesized so far for use as MRI contrast agents.

Ultra small metal oxide nanoparticles synthesized in this work include iron oxide, manganese oxide, and gadolinium oxide nanoparticles, which are coated with various hydrophilic and biocompatible ligands. We tested them for use as MRI contrast agents by measuring the relaxivities. For the first time, these nanoparticles have been applied to molecular MR imaging in rats with a brain tumor.

A key part of the one-pot synthesis is the use of polar organic solvents and air as the oxygen source for metal oxide formation. Both the metal salt as a metal precursor and the biocompatible ligand as a surface-coating ligand are all soluble in polar organic solvents. Air enables the slow formation of the metal oxide nanoparticles. The final products are hydrophilic and biocompatible ligand-coated *ultra small* metal oxide nanoparticles with nearly monodisperse particle diameters. An immediate water solubility of the products makes biomedical applications easy.

Results and Discussion

The HRTEM micrographs show that ligand-coated *ultra small* metal oxide nanoparticles are nearly monodisperse in diameter with average particle diameters that range from 1–3 nm (Figure 1 and Table 1).

Crystal structures of the ligand-coated *ultra small* metal oxide nanoparticles were estimated from lattice fringes (Figure 1 and Table 1). The observed lattice fringes are slightly contracted relative to those of the bulk material because of their *ultra small* size.[15] Lattice distances (L) were estimated by using nanoparticles with good lattice fringes; not all nanoparticles presented good lattice fringes because of their *ultra small* size. For the iron oxide nanoparticles, the measured lattice distances indicate that they are most likely L_{311}

[a] Department of Chemistry, College of Natural Sciences, Kyungpook National University,
Taegu 702-701, South Korea
Fax: +82-53-950-6330
E-mail: ghlee@mail.knu.ac.kr
[b] Department of Nanoscience and Nanotechnology, Kyungpook National University,
Taegu 702-701, South Korea
[c] Department of Diagnostic Radiology, School of Medicine, Kyungpook National University and Hospital,
Taegu 702-701, South Korea
E-mail: ychang@knu.ac.kr
Supporting information for this article is available on the WWW under http://dx.doi.org/10.1002/ejic.200900173.

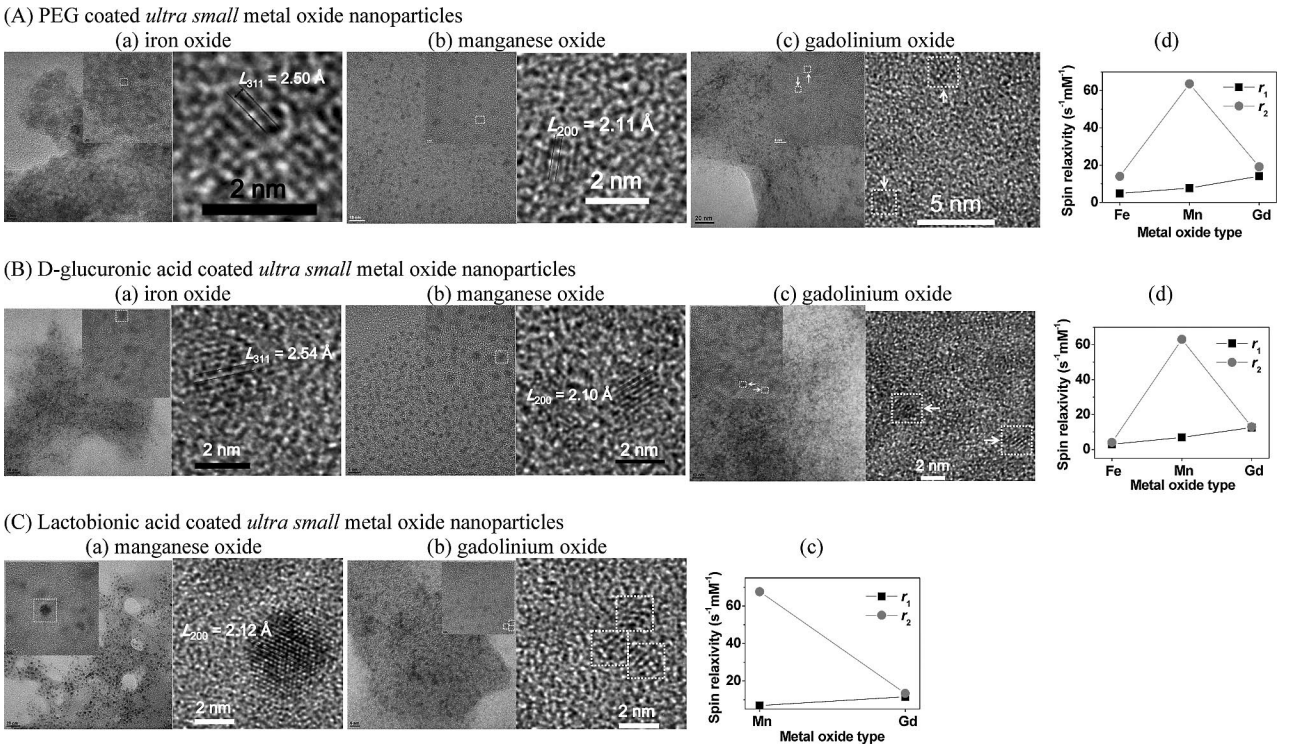

Figure 1. HRTEM micrographs of (A) polyethylene glycol diacid (PEG) coated *ultra small* (a) iron oxide, (b) manganese oxide, and (c) gadolinium oxide nanoparticles; (B) D-glucuronic acid coated *ultra small* (a) iron oxide, (b) manganese oxide, and (c) gadolinium oxide nanoparticles; and (C) lactobionic acid coated *ultra small* (a) manganese oxide and (b) gadolinium oxide nanoparticles. In common from (A) to (C), the square dotted areas in each HRTEM micrograph in the left-hand side figure are magnified and shown in the right-hand side figure. The r_1 and r_2 relaxivities of the *ultra small* metal oxide nanoparticles vs. metal oxide type are plotted for comparison: (A)d PEG coated, (B)d D-glucuronic acid coated, and (C)c lactobionic acid coated.

Table 1. The reaction conditions, the average particle diameters ($d_{av.}$), the r_1 and the r_2 relaxivities, the crystal structures, the magnetic states with blocking temperatures (T_B) in the case of superparamagnetic nanoparticles, and the magnetizations (M) at H = 5 T.

Metal oxide type	Surface coating ligand	Reaction conditions			$d_{av.}$ [nm]	Relaxivity [s^{-1} mM^{-1}]			Crystal structure	Magnetic properties	
		Solvent volume [mL]	Reaction time [h]	Reaction temperature [°C]		r_1	r_2	r_2/r_1		Magnetic state (T_B [K])	M [emu/g]
Fe	PEG	30	24	250	1.9	4.89	14.04	2.87	fcc Fe_3O_4 or fcc γ-Fe_2O_3	Superparamagnetic (25)	5.25
Mn	PEG	30	48	250	1.4	7.75	63.61	8.21	fcc MnO	Paramagnetic	1.49
Gd	PEG	80	72	250	0.9	14.18	19.15	1.35	Amorphous or bcc Gd_2O_3	Paramagnetic	4.52
Fe	D-glucuronic acid	40	12	260	1.5	2.97	4.03	1.36	fcc Fe_3O_4 or fcc γ-Fe_2O_3	Superparamagnetic (≈ 5)	3.85
Mn	D-glucuronic acid	40	24	260	1.5	6.95	63.04	9.07	fcc MnO	Paramagnetic	8.13
Gd	D-glucuronic acid	40	24	260	1.0	12.56	12.95	1.03	Amorphous or bcc Gd_2O_3	Paramagnetic	6.15
Mn	lactobionic acid	40	24	260	1.9	6.90	67.66	9.80	fcc MnO	Paramagnetic	9.20
Gd	lactobionic acid	40	24	260	0.9	11.57	13.38	1.16	Amorphous or bcc Gd_2O_3	Paramagnetic	5.06

of either Fe_3O_4 or γ-Fe_2O_3. It is impossible to distinguish between Fe_3O_4 and γ-Fe_2O_3 in the case of *ultra small* nanoparticles because they possess the same face-centered cubic (fcc) structure with a similar packing.[16] For the manganese oxide nanoparticles, the measured lattice distances indicate that they are most likely L_{200} of fcc MnO. For the gadolinium oxide nanoparticles, only Gd_2O_3 exists because of the electronic configuration ($4f^75d6s^2$) of the Gd atom.[17] Their particle diameters are, however, so small (approximately 1.0 nm) that the lattice distances are hardly measurable for the majority because their lattice fringes are generally poor. We therefore assigned them as amorphous Gd_2O_3. Only a

few, such as that seen in Figure 1 [right-hand side of sample (B)c], however, show a lattice distance of 3.02 ± 0.10 Å, which is most likely L_{222} of body-centered cubic (bcc) Gd_2O_3.

The ligand coatings of the metal oxide nanoparticles were characterized by FTIR spectroscopy. In the FTIR spectra, the observed absorption frequencies characteristic of the ligands include the C–H stretch at ≈2990 cm^{-1}, the C=O stretch at ≈1640 cm^{-1}, and the C–O stretch at ≈ 1110 cm^{-1}. Bonding structures between either amino acid or dicarboxylic acid groups and metal oxide nanoparticles has been spectroscopically well characterized by other groups.[18–21] According to their results, the oxygen atoms of the carboxylic group chemically bind to the surface metal ions, which can be confirmed by the redshifted C=O stretches. Note that the C=O stretches of the surface coating ligands used in this work, i.e. PEG, D-glucuronic acid, and lactobionic acid, occur at ≈1745, ≈1710, and ≈1740 cm^{-1}, respectively (see Supporting Information).

Magnetic properties were investigated and both the *M* vs. T and the *M* vs. *H* curves show that the ligand-coated *ultra small* iron oxide nanoparticles are superparamagnetic at room temperature, whereas both the manganese oxide and gadolinium oxide nanoparticles are paramagnetic at room temperature (Table 1). In the case of the iron oxide nanoparticles, the observed magnetizations at $H = 5$ T are much smaller than the bulk saturation magnetizations of Fe_3O_4 (84 emu/g) and γ-Fe_2O_3 (74 emu/g).[22] We attribute this to the *ultra small* size of the iron oxide nanoparticles in which the surface Fe ion spins are deteriorated by the ligands, as also observed by Yaacob et al.[23]

To test the possibility of using the ligand-coated *ultra small* metal oxide nanoparticles as MRI contrast agents, the longitudinal r_1 and the transverse r_2 relaxivities and the longitudinal T_1 and the transverse T_2 map images were measured. The obtained r_1 and r_2 relaxivities are plotted in Figure 1 to highlight the difference in magnitude between the ligand-coated *ultra small* iron oxide, manganese oxide, and gadolinium oxide nanoparticles and are also provided in Table 1. Both the T_1 and the T_2 map images clearly show dose-dependent contrast changes, respectively (see Supporting Information). Reasonable or high values in the r_1 and the r_2 relaxivities and the clear dose-dependent contrast changes in the T_1 and the T_2 map images suggest that the ligand-coated *ultra small* metal oxide nanoparticles may be used for both/either T_1 and/or T_2 MRI contrast agents. From the measured relaxivities, the order of the ability as T_1 MRI contrast agents is gadolinium oxide > manganese oxide > iron oxide, whereas that as T_2 MRI contrast agents is manganese oxide > gadolinium oxide > iron oxide for the series studied here.

Above all, the r_1 value of the ligand-coated *ultra small* gadolinium oxide nanoparticles is the highest among the metal oxide nanoparticles. This value is consistent with that of gadolinium oxide nanoparticles with larger diameters measured by others.[14] In addition to this, their r_2/r_1 ratio is very close to 1.0 (Figure 1 and Table 1), which indicates that their T_1 MR signal will be maximal because the r_2/r_1 ratio is, in principle, always greater than 1.0.[24] This indicates that the ligand-coated *ultra small* gadolinium oxide nanoparticles will be ideal for T_1 MRI contrast agents. Furthermore, their r_1 value is about three times as high as that (3–5 s^{-1} mM^{-1}) of the clinically used Gd^{3+}-complex T_1 MRI contrast agent.[25,26] This indicates that if they are developed as clinically usable T_1 MRI contrast agents, they will be the most powerful T_1 MRI contrast agents ever known so far. For the moment, they are found to be somewhat toxic[27] (see also Supporting Information for in vitro cytotoxicity test), and thus surface coating needs to be improved.

To confirm the superiority of the ligand-coated *ultra small* gadolinium oxide nanoparticles as T_1 MRI contrast agents, we took 3 T MR images of a rat with a brain tumor. We compared their MR images with those of the manganese oxide nanoparticles. We simply chose the D-glucuronic acid coated *ultra small* gadolinium oxide nanoparticles

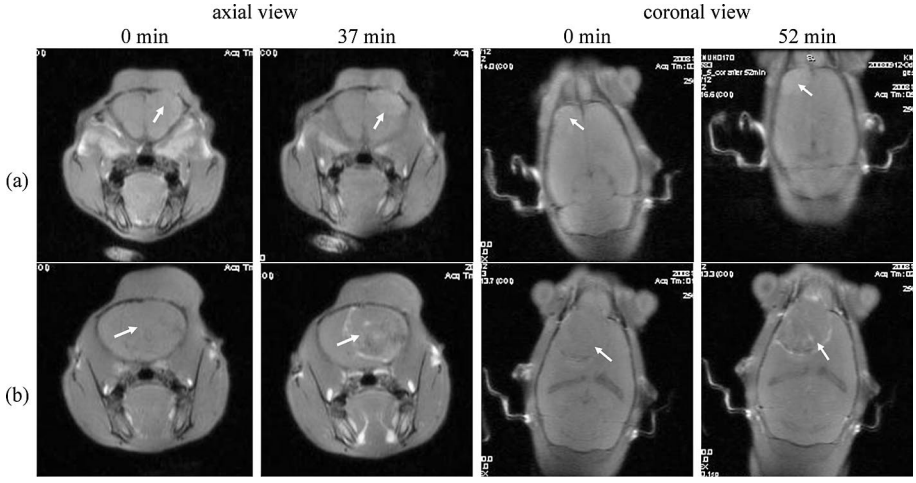

Figure 2. Both axial and coronal 3 T MR images of two different rats with brain tumors (marked by an arrow) before and after injection of (a) sample (B)b (7.31 mM) and (b) sample (B)c (13.47 mM) in Figure 1; 0.957 mL of sample (B)b and 0.2 mL of sample (B)c were injected into the rats.

[sample (B)c in Figure 1] and the D-glucuronic acid coated *ultra small* manganese oxide nanoparticles [sample (B)b in Figure 1] for this purpose. Here, the ligand-coated *ultra small* iron oxide nanoparticles were not considered for comparison because their contrasting ability in MR images will be the poorest because they possess the smallest r_1 relaxivity (Figure 1 and Table 1). To record the MR images, 0.957 mL of the sample (B)b (7.31 mM) and 0.2 mL of the sample (B)c (13.47 mM) were injected into two different rats with brain tumors. Both axial and coronal 3 T MR images taken before and after the injection of the two samples are shown in Figure 2. The T_1 contrast enhancement of the brain tumors (marked by arrows) after injection can clearly be observed in both samples. However, the sample (B)c shows a greater contrast enhancement of the brain tumor than that in sample (B)b, even though the injected amount of sample (B)b (7.0 mmol Mn) is about 2.6 times larger than that of sample (B)c (2.7 mmol Gd). This result proves the superiority of the ligand-coated *ultra small* gadolinium oxide nanoparticles.

Conclusions

In summary, we developed the synthesis for nanotechnology-based high-performance MRI contrast agents, which are aimed for both highly sensitive and target-specific molecular MR imaging. The nanoparticles include hydrophilic and biocompatible ligand-coated *ultra small* iron oxide, manganese oxide, and gadolinium oxide nanoparticles with average particle diameters ($d_{av.}$) that range from 1–3 nm and with reasonable or high r_1 and r_2 relaxivities. Above all, we found that the ligand-coated *ultra small* gadolinium oxide nanoparticles are suitable as T_1 MRI contrast agents: the very high r_1 relaxivity, which is about three times as high as that of the clinically used Gd^{3+}-complex T_1 MRI contrast agent (the result of nanotechnology), and the value for the r_2/r_1 ratio that is very close to 1.0. Their superior performance as T_1 MRI contrast agents was proved through in vivo T_1 MR images of a rat with a brain tumor.

Experimental Section

Chemicals used in the synthesis include triethylene glycol as a solvent, $FeCl_3{\cdot}6H_2O$ (or $MnCl_2{\cdot}4H_2O$ or $GdCl_3{\cdot}6H_2O$) as a metal precursor, polyethylene glycol diacid (PEG) ($M_n \approx 600$) (or D-glucuronic acid or lactobionic acid) as a surface coating ligand, and air (a mixture of 21% O_2 and 79% N_2) as an oxygen source. The chemicals were all purchased from Aldrich and used as received. The air was purchased from a local distributor and used after the moisture was removed. For all reactions, 5 mmol of a metal salt and 5 mmol of a ligand were used, which were then added to 30–80 mL of triethylene glycol. The mixture was heated to 100 °C while magnetically stirred and was maintained at that temperature until both the metal salt and the ligand were completely dissolved in the triethylene glycol solvent. The mixture was then heated at reflux at 250–260 °C for 12–72 h, while air was bubbled through. The exact reaction conditions (i.e. solvent volume, reaction temperature, and reaction time) used for the synthesis of each of the ligand-coated *ultra small* metal oxide nanoparticles are provided in Table 1. It was noticed that the reaction conditions differ slightly depending on ligand species used. After the reaction, the mixture was cooled to room temperature and diluted with deionized water for the MRI experiment. To obtain a powder sample, acetone was added to the reaction mixture. The top solution was decanted and the remaining precipitate was dried in air.

Particle diameters were measured with a high resolution transmission electron microscope (HRTEM) at acceleration voltages of 200 kV (JEOL, JEM 2100F). Ligand coatings of *ultra small* metal oxide nanoparticles were characterized with a Fourier transform infrared (FTIR) absorption spectrometer (Mattson Instruments, Inc., Galaxy 7020A) (see Supporting Information). To record the FTIR absorption spectra, pellets were made by pressing mixtures of each of the powder samples and KBr. The magnetic properties were measured with a superconducting quantum interference device (SQUID) magnetometer (Quantum Design, MPMS-7). Net masses of the metal oxide nanoparticles in ligand-coated metal oxide nanoparticles were estimated with a thermogravimetric analyzer (TGA) (TA Instruments, SDT Q 600) (see Supporting Information) and used to correct magnetizations. Both hysteresis loops (M vs. H curves) ($-5 \leq H \leq 5$ T) at a temperature of 300 K and zero-field-cooled (ZFC) magnetization vs. temperature curves (M vs. T curves) ($3 \leq T \leq 330$ K) at an applied field of 100 Oe were recorded (see Supporting Information). The longitudinal r_1 and the transverse r_2 relaxivities and the longitudinal T_1 and the transverse T_2 map images were measured with an MRI instrument (GE 1.5 T, Excite) equipped with the Knee coil (EXTREM). Both the sample preparation and the data acquisition followed the same experimental procedure described previously.[13] MR images (3 T) of a rat with a brain tumor were taken with an MRI instrument (GE 3 tesla, Signa HD).

Supporting Information (see footnote on the first page of this article): FTIR spectra, TGA curves, M vs. H curves, zero-field-cooled (ZFC) M vs. T curves, T_1 map images, T_2 map images, and the in vitro cytotoxicity test are presented.

Acknowledgments

This project was supported by the Regional Technology Innovation Program of the Ministry of Commerce, Industry, and Energy funded by the Korean Government by a Grant (No. RTI04-01-01) and by the Korea Research Foundation Grant funded by the Korean Government (KRF-2008-313-C00416). We thank the Korea Basic Science Institute for allowing us to use their HRTEM.

[1] T. Shen, R. Weissleder, M. Papisov, A. Bogdanov, T. J. Brady, *Magn. Reson. Med.* **2005**, *29*, 599–604.
[2] P. Wunderbaldinger, L. Josephson, R. Weissleder, *Acad. Radiol.* **2002**, *9*, S304–S306.
[3] R. Weissleder, D. D. Stark, B. L. Engelstad, B. R. Bacon, C. C. Compton, D. L. White, P. Jacobs, J. Lewis, *AJR Am. J. Roentgenol.* **1989**, *152*, 167–173.
[4] S.-J. Cho, B. R. Jarrett, A. Y. Louie, S. M. Kauzlarich, *Nanotechnology* **2006**, *17*, 640–644.
[5] C. Billotey, C. Wilhelm, M. Devaud, J. C. Bacri, J. Bittoun, F. Gazeau, *Magn. Reson. Med.* **2003**, *49*, 646–654.
[6] C. Chapon, F. Franconi, L. Lemaire, L. Marescaux, P. Legras, J. P. Saint-André, B. Denizot, J.-J. Jeune, *Invest. Radiol.* **2003**, *38*, 141–146.
[7] L. X. Tiefenauer, A. Tschirky, G. Kühne, R. Y. Andres, *Magn. Reson. Imaging* **1996**, *14*, 391–402.
[8] C. W. Jung, P. Jacobs, *Magn. Reson. Imaging* **1995**, *13*, 661–674.

[9] D. J. Widder, W. L. Greif, K. J. Widder, R. R. Edelman, T. J. Brady, *Am. J. Radiol.* **1987**, *148*, 399–404.
[10] H. Lee, M. K. Yu, S. Park, S. Moon, J. J. Min, Y. Y. Jeong, H.-W. Kang, S. Jon, *J. Am. Chem. Soc.* **2007**, *129*, 12739–12745.
[11] H. B. Na, J. H. Lee, K. An, Y. I. Park, M. Park, I. S. Lee, D.-H. Nam, S. T. Kim, S.-H. Kim, S.-W. Kim, K.-H. Lim, K.-S. Kim, S.-O. Kim, T. Hyeon, *Angew. Chem. Int. Ed.* **2007**, *46*, 5397–5401.
[12] J.-H. Lee, Y.-M. Huh, Y. Jun, J. Seo, J. Jang, H.-T. Song, S. Kim, E.-J. Cho, H.-G. Yoon, J.-S. Suh, J. Cheon, *Nature Medicine* **2007**, *13*, 95–99.
[13] J. Y. Park, P. Daksha, G. H. Lee, S. Woo, Y. Chang, *Nanotechnology* **2008**, *19*, 365603 (7pp).
[14] a) M.-A. Fortin, R. M. Petoral, F. Söderlind, A. Klasson, M. Engström, T. Veres, P.-O. Käll, K. Uvdal, *Nanotechnology* **2007**, *18*, 395501 (9pp); b) M. Engström, A. Klasson, H. Pedersen, C. Vahlberg, P.-O. Käll, K. Uvdal, *Magn. Reson. Mater. Phys.* **2006**, *19*, 180–186.
[15] For example, see W. Vogel, B. Rosner, B. Tesche, *J. Phys. Chem.* **1993**, *97*, 11611–11616.
[16] R. M. Cornell, U. Schwertmann, *The Iron Oxides*, VCH, Weinheim, **1996**, pp. 28–31.
[17] F. A. Cotton, G. Wilkinson, *Advanced Inorganic Chemistry*, *4th ed.*, John Wiley & Sons, New York, **1980**, pp. 981–983.
[18] C. B. Mendive, T. Bredow, M. A. Blesa, D. W. Bahnemann, *Phys. Chem. Chem. Phys.* **2006**, *8*, 3232–3247.
[19] S. J. Hug, D. Bahnemann, *J. Electron Spectrosc. Relat. Phenom.* **2006**, *150*, 208–219.
[20] O. W. Duckworth, S. C. Martin, *Geochim. Cosmochim. Acta* **2001**, *65*, 4289–4301.
[21] A. D. Roddick-Lanzilotta, A. J. McQuillan, *J. Colloid Interface Sci.* **1999**, *217*, 194–202.
[22] R. C. O'Handley, *Modern Magnetic Materials, Principles and Applications*, John Wiley & Sons, Inc., New York, **2000**, p. 125.
[23] I. I. Yaacob, A. C. Nunes, A. Bose, *J. Colloid Interface Sci.* **1995**, *171*, 73–84.
[24] The r_2/r_1 relaxivity ratio is always greater than 1.0 because the T_2/T_1 spin relaxation time ratio is always less than 1.0. see R. H. Hashemi, W. G. Bradley, C. J. Lisanti, *MRI: The Basics*, *2nd ed.*, Lippincott Williams & Wilkins, Philadelphia, **2004**, pp. 42–43.
[25] P. Caravan, J. J. Ellison, T. J. McMurry, R. B. Lauffer, *Chem. Rev.* **1999**, *99*, 2293–2352.
[26] For instance, the Gd^{3+}-complex T_1 contrast agents clinically used in hospital include Magnevist (Bayer HealthCare, http://www.schering-diagnostics.de) and Omniscan (GE Healthcare, http://md.gehealthcare.com), etc.
[27] The rats into which 0.957 mL of sample (B)b (7.31 mM) and 0.2 mL of sample (B)c (13.47 mM) in Figure 1 were injected survived for ≈24 and ≈10 h after injection, respectively.

Received: February 19, 2009
Published Online: April 29, 2009

